Cross-Strain Quorum Sensing Inhibition by Staphylococcus Aureus. Part 2: A Spatially Inhomogeneous Model

Jabbari, Sara; King, John R.; Williams, Paul

DOI:
10.1007/s11538-011-9702-0

Document Version
Peer reviewed version

Citation for published version (Harvard):
Jabbari, S, King, JR & Williams, P 2012, 'Cross-Strain Quorum Sensing Inhibition by Staphylococcus Aureus. Part 2: A Spatially Inhomogeneous Model', *Bulletin of Mathematical Biology*, vol. 74, no. 6, pp. 1326-1353. https://doi.org/10.1007/s11538-011-9702-0

Cross-strain quorum sensing inhibition by *Staphylococcus aureus*. Part 2: a spatially inhomogeneous model.

Sara Jabbari, John R. King

Centre for Mathematical Medicine and Biology, School of Mathematical Sciences, University of Nottingham, Nottingham, NG7 2RD, UK

Paul Williams

School of Molecular Medical Sciences, University of Nottingham, Nottingham, NG7 2RD, UK

September 6, 2011

The final publication is available at http://link.springer.com/article/10.1007/s11538-011-9702-0

Abstract

Staphylococcus aureus uses quorum sensing (QS) to enhance its pathogenicity. An intriguing aspect of this is that different strains are capable of inactivating the QS systems of opposing strains. In Part 1 of this study we presented a model of this phenomenon in a well-mixed environment; here we incorporate spatial structure. Two competitive strains occupying adjacent habitats with freely diffusing QS signal molecules (QSSMs) are considered. We investigate the effect of the QSSM diffusion coefficient and the relative size of the two populations on the ability of one population to dominate the other. Regarding population size, a larger population is generally at an advantage (initial conditions permitting), while the implications of different diffusivities are more complex and depend upon the sizes of the populations.

Keywords: gene regulation networks, mathematical modelling, quorum sensing, reaction-diffusion equations, *Staphylococcus aureus*.

1 Introduction

Quorum sensing (QS) is a cell-cell communication mechanism used by many species of bacteria enabling a bacterial cell to coordinate its behaviour in conjunction with its population size or density; for reviews of this mechanism see, for example, [1, 2] or [3]. In brief, each cell within a population exports a quorum sensing signal molecule (QSSM) across its membrane(s). Extracellular QSSMs can then be detected, either by binding to receptors located on the cell membrane (usually the case for Gram-positive bacteria), or to intracellular receptors (Gram-negative bacteria). QSSMs need not necessarily be produced by the same cell which detects them, and thus a means of cell-cell communication emerges. The traditional view of QS is that the more cells that are present, the more QSSMs in the extracellular environment, such that each cell can effectively titrate its population size. More recently, the alternative view of 'diffusion sensing' (DS) [4] has been put forward, whereby it is suggested that QS allows a cell to recognise its environment rather than its population size, i.e. the environment will affect the QSSM diffusion coefficient: the denser the environment the more QSSMs will be retained in the surroundings of the cell. Thus the cell can alter its behaviour according to its environment. The names 'efficiency' [5] and 'positional' [6] sensing capture the possibility that QSSMs can monitor both population size and environmental conditions, depending upon the situation.

QS systems can be manipulated for a wide range of purposes and a variety of QS systems exist in different bacteria, indeed some species use multiple systems in parallel. *Staphylococcus aureus* is a Gram-positive bacteria which uses the *agr* QS system to collectively co-ordinate virulence [7], both in terms of the classical view of QS and the less conventional DS. While its population size is small, *S. aureus* produces surface proteins which facilitate adherence to host tissues and aid immune evasion through uptake into host epithelial and endothelial cells. As the population grows, a switch to the production of secreted virulence factors occurs, leading to the damage and degradation of the surrounding host cells and tissues, thus actively attacking the host. Since tissue damage will alert host defence systems, such a delayed 'deployment tactic' may allow the infecting bacteria time to reach a sufficient population size to be able to overwhelm the host [8]. However, the *agr* system is also used for DS. For instance, a single *S. aureus* cell can become internalised within the endosome of a host cell. Its QSSM, termed an auto-inducing peptide (AIP), builds up inside the host cell triggering activation of the *agr* genes. This results in production of the appropriate virulence factors (notably alpha-toxin) which facilitate

endosome escape (for a mathematical model of this process see [9]). Thus here, the system is being used to sense the cell's environment, its population size being irrelevant.

Despite the variety of QS systems which have been discovered, many bacteria are able to interact with systems from other species or strains. For example, *Pseudomonas aeruginosa* is a Gram-negative bacterium using a QS system unrelated to that of *S. aureus* but one of its QSSMs, namely 3-oxo-C12-HSL, interferes with the production of certain *agr*-regulated virulence factors in *S. aureus* [10]. A particularly interesting phenomenon in *S. aureus* is that all the strains of *S. aureus* can be divided into four distinct *agr* groups (I-IV), and in general we see cross-activation of *agr* systems of strains within a group and cross-inhibition with strains from other groups [11]. The sequencing of large numbers of bacterial genomes has revealed that *agr*-type QS systems are conserved in many more Gram-positive bacterial species, including the pathogens *Clostridium botulinum* [12], *Clostridium perfringens* [13], *Enterococcus faecelis* [14] and *Listeria monocytogenes* [15]. Thus, while the implications of this study are discussed principally in relation to *S. aureus*, the results are more widely relevant, with cross-species *agr* signalling being likely to occur.

The emergence of antibiotic-resistant strains of *S. aureus* has made the development of new therapies to combat staphylococcal infections increasingly urgent. Given its use in pathogenicity, it is clear that understanding the QS system in *S. aureus* could provide insight into such therapies. For example, it should be possible to produce a non-pathogenic strain which could be used to downregulate the *agr* system of an infecting strain, thus attenuating it and leaving the immune system capable of dealing with the infection. Indeed, in mice, *S. aureus* skin abscess infections caused by a strain producing AIP-1 can be prevented by coadministering an AIP-2 [16]. Since the therapy would not directly kill the bacteria, the chance of resistance developing is greatly reduced (though not eradicated) in comparison with antibiotic treatment where cells develop resistance to survive [17].

In Part 1 of this study [18] we examined cross-strain QS inhibition by two populations of *S. aureus* that are assumed to be in a well-mixed environment and therefore spatially homogeneous. While this is a reasonable assumption under certain circumstances, for example in a chemostat, it is desirable to extend the model to account for circumstances where spatial effects are important and the populations are non-uniform. To our knowledge, although spatially-structured models of QS by Gram-negative bacteria exist, see for example [6, 19], no spatially heterogeneous models of Gram-positive QS have so far been published. In this study we focus

on the scenario of two distinct strains of *S. aureus* (from opposing groups) being positioned adjacent on a horizontal surface, this representing a simple situation in which to start to analyse the implications of spatial variations. Each produces (competitive) diffusible QSSMs that mediate communication within and between the two populations.

The model we present here is a simplified version of our existing cross-strain model incorporating a classical two component system (TCS), i.e. Model I from [18], but with spatial dependence now included. Details of the simplification are outlined in the appendix, and stem from the asymptotic analyses of the steady states presented in [20], where we examined the response of a single strain to virulence inhibition by synthetic AIP. By altering the relative population size of two competing strains in the present study, we are able to demonstrate the ability of one strain to downregulate the *agr* system of the other. With a view to examining the capabilities of a recombinant non-pathogenic strain of *S. aureus* to inactivate the virulence of an infecting strain, we examine the effect of altering the diffusion coefficient of the AIPs.

2 A spatially structured model

2.1 Model formulation

The *agr* operon (see, for example, [7]) consists of two transcription units (*agrBDCA* and RNAIII respectively) that are driven by regulatory proteins which bind to promoters termed P2 and P3, permitting RNA polymerase to transcribe the DNA into mRNA, prior to translation of this *agr* mRNA into proteins. The P2 transcript consists of four genes which are transcribed and translated to give four proteins (AgrB, AgrD, AgrC and AgrA), see Figure 1. AgrB is a transmembrane protein and is involved in the post-translational conversion of the AgrD pro-peptide into the AIP (the QSSM of the system). The AIP is secreted into the external environment where it is detected by a receptor protein (AgrC) present on the bacterial cell surface. AIP binding to AgrC induces a phosphorylation/dephosphorylation cascade which results in the activation of AgrA, a DNA-binding protein which interacts with both the P2 and P3 promoters. AgrA and AgrC are, respectively, the response regulator and sensor kinase of a TCS. For the purposes of this model we assume that this is a classical TCS, i.e. the phosphorylation cascade occurs as follows: upon binding to AIP, AgrC autophosphorylates before transferring

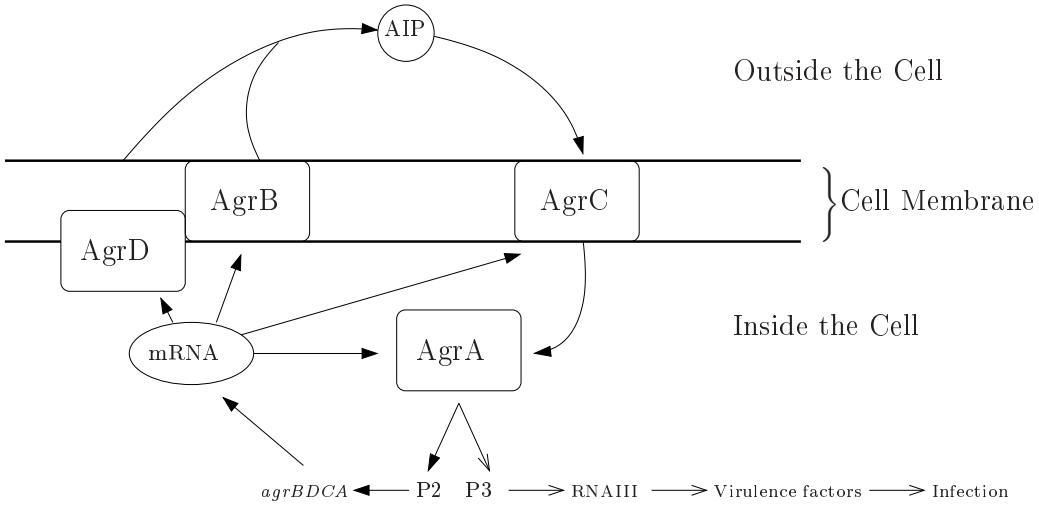

Figure 1: A schematic of the *agr* feedback loop. The arrows with a filled head illustrate the positive feedback loop. In Figure 2 we illustrate the simplified version of this network which we use to create the spatially structured model.

the phosphate to AgrA. Phosphorylated AgrA binds to the DNA, causing upregulation of both the P2 and P3 promoters. This corresponds to Model I of [18]. Upregulation of the P3 promoter results in increased secreted virulence factor production, while upregulation of the P2 promoter induces higher transcription of the *agr* mRNA, thus completing the positive feedback loop which forms this QS system, i.e. AIP generation drives the synthesis of further AIPs.

In Part 1 of this study [18] we presented a spatially homogeneous model of cross-strain inhibition between two strains of *S. aureus*. We now simplify this model through an asymptotic analysis of its steady states and extend it to incorporate spatial variations. In the interests of brevity, details of the nondimensionalisation can be found in [18] while those of the simplification are relegated to the appendix; we summarise both here (and further details can be obtained from [21]).

The nondimensionalisation arises from scaling of the relevant variables by their down-regulated steady state values. Nondimensionalisations of the remaining variables (i.e. those which have a zero down-regulated steady state) are chosen to set as many parameters as possible to be unity (specifically, the coefficients of basal mRNA transcription, AIP-receptor binding, AgrA activation and phosphorylated AgrA binding to the promoter site in certain equations). Since insufficient data are available for full parametrisation of the model, we set ourselves

up to exploit asymptotic techniques: parameters are scaled according to the small parameter ϵ which represents the ratio of basal mRNA transcription to QS-induced transcription of mRNA (the smallness of which is implicit in the concept of QS itself). All parameter values follow directly from [18]. Simplification of the model is based upon the systematic asymptotic analysis (see Appendix A) of the possible steady states (giving both populations as up-regulated or either population downregulating the other). If the component of the steady state for a particular variable is the same for all steady states, that variable is set to be at quasi-steady state. If a particular term does not appear at leading order in any steady state, it is neglected from the model. Thus, at steady state, with our parameter choice, all results should reproduce those of the full model (for sufficiently small ϵ). Simplification of the model can be summarised as follows:

- binding and activation reactions are relatively fast, so that AIP-bound receptors and phosphorylated AgrA are taken to be at quasi-steady state;
- housekeeping dephosphorylation of AgrA can be disregarded as it is negligible in relation to either natural depletion or phosphorylation of AgrA;
- AIP binding to, and separation from, AgrC is negligible in relation to production and degradation of this QSSM;
- degradation of transmembrane AgrC can be neglected in favour of its binding reactions.

The resulting simplified network is outlined in Figure 2 (contrast with Figure 1). The required variables and parameters (along with the default parameter choice) are displayed in Tables 1 and 2 respectively.

We assume uniform layers of cells of each population are placed side by side on the interval $0 \leq x \leq W$, so that Population 1 occupies $0 \leq x \leq W/2$ and Population 2 lies in $W/2 \leq x \leq W$, see Figure 3. We suppose that the AIP molecules are free to diffuse among the two populations (with diffusion coefficients D_1 and D_2 for the respective AIPs) while the bacterial populations remain approximately stationary; thus only the differential equations representing the signal molecules require spatial derivatives. Note that if we assume both populations reside across the entire interval $0 \leq x \leq W$ we get results analogous to the well-mixed model of [18]. Nondimensionalisations follow from [18] and are detailed in the appendix with the addition of

$$x' = \frac{x}{W}, \qquad {D_1}' = \frac{D_1}{\delta_M W^2}, \qquad {D_2}' = \frac{D_2}{\delta_M W^2},$$

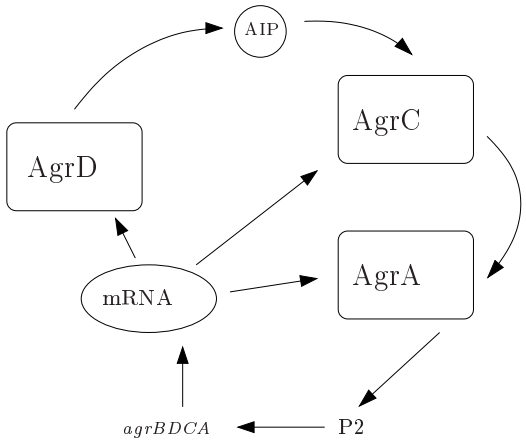

Figure 2: A schematic of the simplified version of the *agr* feedback loop used to build the spatial model. In Figure 1 we illustrate the full network.

Nondimensional variable	Interpretation
M_j	mRNA in population j
A_j	cytoplasmic AgrA in population j
R_j	transmembrane AgrC in population j
S_j	anchored AgrD in population j
a_j	free AIP in population j
P_j	proportion of cells that is up-regulated in population j

Table 1: Definitions of the variables, $j = 1, 2$.

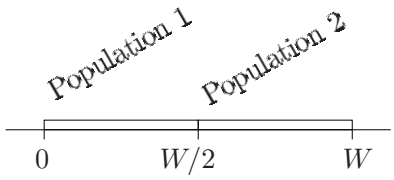

Figure 3: Schematic of the competing populations of *S. aureus*, positioned side by side. For definiteness we take each to be of the same extent, $W/2$.

Nondimensional parameter	Interpretation	Default Value
k_S	AgrD loss through AIP production	10^{-1}
η	Receptor loss through AIP binding	10^{-1}
λ	natural protein degradation	1
λ_a	natural AIP degradation	1
γ_{jl}	AIP from Population j separating from Population l receptor	1
ϕ	activation of AgrA	1
u	unbinding of active AgrA from the DNA binding site	1
β_A	ratio of cognate AIP binding in Population 2 to Population 1	1
β_I	ratio of AIP from Population 1 binding to Population 2 receptors, to AIP from Population 2 binding to Population 1 receptors	1
v	ratio of activated *agr* transcription to basal transcription	10
β_{jl}	binding of AIP from Population j to receptors of Population l	10
k_a	AIP production	10^2
N	ratio of the size of Population 1 to Population 2	-
D_j	diffusion coefficient of AIP from Population j $(j = 1, 2)$	-
ϵ	ratio of basal to QS-induced transcription	10^{-1}

Table 2: Interpretation of the dimensionless parameters and their default values with $j = 1, 2$ and $l = 3 - j$. Notice that we have not specified the values of N, D_1 or D_2 as in this paper we focus on the effects of varying these three parameters.

so that x is scaled with the interval width. One significant parameter is the ratio of the two population sizes:

$$N = \frac{N_1}{N_2}; \tag{1}$$

we shall investigate the influence of this parameter upon the results of the model. The nondimensional variables are defined on $0 \leq x' \leq 1$ and, dropping primes, we have

$$\frac{\partial M_1}{\partial \tau} = \frac{1}{\epsilon}\hat{\upsilon}P_1 - M_1 + 1, \quad 0 \leq x \leq 1/2, \tag{2}$$

$$\frac{\partial A_1}{\partial \tau} = \lambda(M_1 - A_1) - \frac{\phi A_1 R_1 a_1}{(\lambda + \gamma_1)}, \tag{3}$$

$$\frac{\partial S_1}{\partial \tau} = \lambda(M_1 - S_1) - \epsilon\hat{k}_S M_1 S_1, \tag{4}$$

$$\frac{\partial a_1}{\partial \tau} = \frac{1}{\epsilon^2}\hat{k}_a M_1 S_1 - \lambda_a a_1 + D_1\frac{\partial^2 a_1}{\partial x^2}, \tag{5}$$

$$\frac{\partial R_1}{\partial \tau} = \lambda M_1 - \epsilon\frac{\hat{\eta}\lambda}{(\lambda + \gamma_{11})}R_1 a_1 - \epsilon\frac{N\hat{\beta}_{21}\hat{\eta}\lambda}{\hat{\beta}_{11}\beta_A(\lambda + \gamma_{21})}R_1 a_2, \tag{6}$$

$$\frac{\partial P_1}{\partial \tau} = \frac{A_1 R_1 a_1}{\lambda(\lambda + \gamma_{11})}(1 - P_1) - uP_1, \tag{7}$$

$$\frac{\partial M_2}{\partial \tau} = \frac{1}{\epsilon}\hat{\upsilon}P_2 - M_2 + 1, \quad 1/2 \leq x \leq 1, \tag{8}$$

$$\frac{\partial A_2}{\partial \tau} = \lambda(M_2 - A_2) - \frac{\phi}{(\lambda + \gamma_2)}A_2 R_2 a_2, \tag{9}$$

$$\frac{\partial S_2}{\partial \tau} = \lambda(M_2 - S_2) - \epsilon\frac{\hat{k}_S}{N}M_2 S_2, \tag{10}$$

$$\frac{\partial a_2}{\partial \tau} = \frac{1}{\epsilon^2}\frac{\hat{k}_a\hat{\beta}_A}{N^3}M_2 S_2 - \lambda_a a_2 + D_2\frac{\partial^2 a_2}{\partial x^2}, \tag{11}$$

$$\frac{\partial R_2}{\partial \tau} = \lambda M_2 - \epsilon\frac{N\hat{\eta}\lambda}{(\lambda + \gamma_{22})}R_2 a_2 - \epsilon\frac{\beta_I\hat{\beta}_{21}\hat{\eta}\lambda}{\hat{\beta}_{11}(\lambda + \gamma_{12})}R_2 a_1, \tag{12}$$

$$\frac{\partial P_2}{\partial \tau} = \frac{A_2 R_2 a_2}{\lambda(\lambda + \gamma_{22})}(1 - P_2) - uP_2, \tag{13}$$

(the hatted parameters are those that have been scaled with ϵ).

We assume AIP to be confined within $0 \leq x \leq 1$, so the boundary conditions are

$$\frac{\partial a_1}{\partial x} = 0, \quad \frac{\partial a_2}{\partial x} = 0, \quad \text{at} \quad x = 0, 1; \tag{14}$$

these are appropriate to some laboratory (at least) conditions. An alternative is that the boundaries are perfect sinks ($a_1 = a_2 = 0$ at $x = 0, 1$) so that AIP is lost to the surroundings: this could arise at an infection site, for example, thus necessitating the production of extra AIPs to reach an active state, leaving a strain more susceptible to inhibition. We shall not, however, investigate this scenario here.

Note that M_1 and M_2 are each defined on half of the domain only. We take other variables to have zero initial data in the range of x in which the corresponding population is absent. Given previous studies which illustrate multistable behaviour by the *agr* operon [20, 22, 23], the initial conditions of the system are likely to be crucial in determining the ability of one population to overcome the other. For example, a population beginning with a higher level of *agr* activity than the other would, all else being equal, be expected to be at an advantage. There are therefore numerous initial conditions which we could examine. As a basis for the current

investigation, we use the following four sets of initial conditions (remembering that here 'down-regulated' refers to a naturally inactive state which would be the result of a sufficiently small population or sufficiently large AIP diffusion coefficient, not a suppressed one).

I.C. I Population 1 begins up-regulated and Population 2 down-regulated.

I.C. II Both Populations begin down-regulated.

I.C. III Population 1 begins down-regulated and Population 2 up-regulated.

I.C. IV Both Populations begin up-regulated.

When a population is required to begin in a naturally down-regulated state we adapt the initial conditions from [18, 22]. So, for example for **I.C. II** we have

$$\begin{aligned} &\text{For} \quad X = A, S, R, \quad X_1(x,0) = \begin{cases} 1, & 0 \le x < 1/2, \\ 0, & 1/2 < x \le 1, \end{cases} \qquad X_2(x,0) = \begin{cases} 0, & 0 \le x < 1/2, \\ 1, & 1/2 < x \le 1, \end{cases} \\ &a_1(x,0) = a_2(x,0) = P_1(x,0) = P_2(x,0) = 0, \qquad 0 \le x \le 1, \\ &M_1(x,0) = 1, \quad 0 \le x < 1/2, \qquad M_2(x,0) = 1, \quad 1/2 < x \le 1. \end{aligned} \tag{15}$$

When a population is specified to begin in an up-regulated state, we use the steady-state values which result when the opposing population is absent under the particular parameter choice in question.

We retain parameter scalings from Part 1 [18], but we now have two new parameters: the diffusion coefficients of the two strains' AIPs. For the most part, we assume that they are equal ($D_1 = D_2 = D$, say) since the bacteria are in the same medium and produce structurally similar signal molecules (Table 3 provides the molecular weights of the different AIP) and examine how this value affects the outcome (Figure 4, for example, illustrates how the distribution of signal molecules is affected by the diffusion constant when $N = 1$). Our numerical investigations indicate two parameter regimes in D, which give distinct phenotypes. To illustrate both of these we select $D = 0.5$ from the regime of larger D and $D = 0.1$ from that of the smaller. In §5.2-5.3 we demonstrate the effect of a wider range of D upon the steady states of the system and, finally, in §5.4, we investigate the consequences of differing diffusivities between the two populations.

	Molecular weight
AIP I	961.11 g/mol
AIP II	878.99 g/mol
AIP III	818.9797 g/mol
AIP IV	1009.1982 g/mol

Table 3: Molecular weights of each of the four different AIP molecules [24].

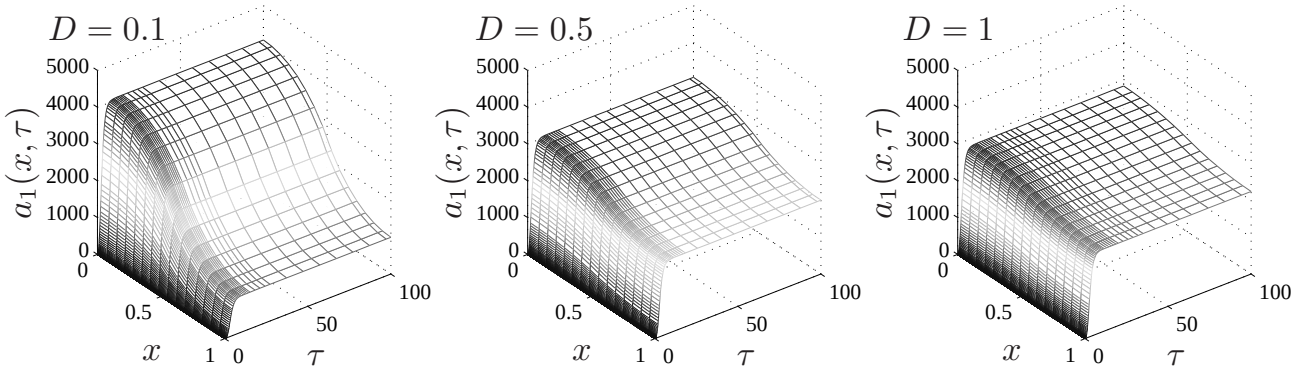

Figure 4: Numerical solutions for $a_1(x,\tau)$ when $N = 1$ for various values of D using initial conditions II and the default parameter set as given by Table 2. Since their population sizes, diffusion coefficients and initial conditions are equal, the corresponding solutions for Population 2 are the same but reflected spatially. As the diffusion constant increases, the AIP profile becomes more uniform as they are able to reach further into the opposition territory, with fewer AIP molecules remaining in the region occupied by the strain producing that AIP. An implication is that, while it is desirable for the bacteria to spread their AIP to the opposition bacteria in order to gain a competitive advantage, they must also retain a sufficient amount to remain up-regulated.

Following Part 1, where it was shown that the key determinant in the ability of one population to downregulate another was their relative population size, N, we describe the effect of varying N for two dimensionless diffusivities that give qualitatively different behaviour. For the numerical solutions, spatial centred discretisation is used to reduce the model into a compartmental one where each compartment is described by a system of ordinary differential equations (ODEs) linked by the centred discretisation of the diffusion terms. The ODEs are then solved in MATLAB v.7.1 (The MathWorks, Inc.) to generate time-dependent solutions or XPPAUT 5.91 to calculate steady-state solution curves.

3 Time-dependent numerical solutions

3.1 Larger diffusion, $D = 0.5$

We begin by considering the time-dependent solutions for each of the four initial conditions when $D = 0.5$, see Figure 5. In each case we see how, for sufficiently large N, i.e. Population 1 is larger than Population 2, the former is able to establish its dominance and the critical value of N at which this is achieved is dependent upon the initial conditions of the system (we shall see in §4 that a bifurcation occurs with varying N which produces this dramatic change in response).

Initial conditions I and II have Population 2 beginning in a down-regulated state. The value of N required to ensure that it remains in this state is distinctly less than that required to push Population 2 into an inactive state when Population 2 begins up-regulated: contrast the results of Figure 5(a)-(b) with the solutions resulting from initial conditions III and IV in (c)-(d). Additionally, for initial conditions I and II, Population 1 gains a clear advantage by already being in an up-regulated state (the critical value for initial condition I is less than that for initial condition II). This scenario could be viewed as the cells delaying the release of their QSSMs to the wider environment until they have already reached an active state (in [18] we illustrated the need for the cells to achieve their own upregulation before attempting to inactivate their competitors). On the other hand, the same critical value of N is required for Population 1 to downregulate Population 2 whether the system begins with initial conditions III or IV (when Population 2 is initially active). This is reflective of the bistable behaviour of the system which we will see in §4: if Population 2 is initially active, the value of N required to

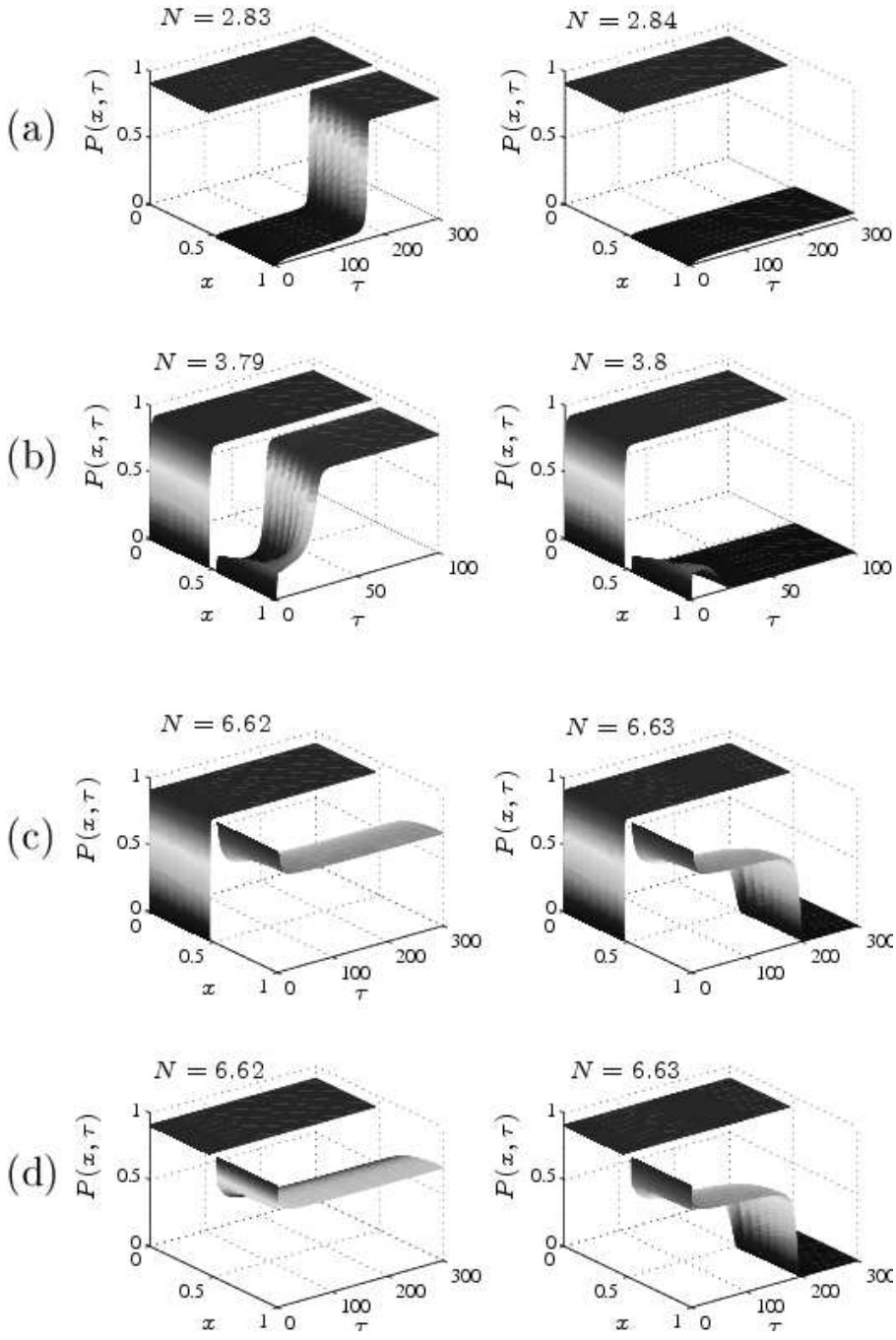

Figure 5: Numerical solutions illustrating the critical values of N needed to enable Population 1 to force Population 2 into an inactive state when $D_1 = D_2 = 0.5$, using the initial conditions (a) I (b) II (c) III and (d) IV. In the left-hand column, Population 1 fails to inactivate Population 2 with the given values of N. In the right-hand column, N is increased sufficiently for Population 1 to succeed in downregulating Population 2.

downregulate this population corresponds to the location of the fold bifurcation on the upper section of the two bifurcation curves (we refer the reader forward to Figure 8), regardless of the initial conditions of Population 1.

We also see from Figure 5(c)-(d) that, for these initial conditions (whereby Population 2 begins in an up-regulated state), there exists a range of N where, while Population 2 cannot be deemed to be in an inactive state, its proportion of up-regulated cells is markedly smaller than that of Population 1: although Population 1 can be said to be having a clear effect on its opponent, it is not sufficient to establish absolute control. The spatial inhomogeneity of the individual populations is clearly evident here, as the Population 2 bacteria nearest the centre of the interval ($x = 0.5$) have a lower regulation level than those at the extremity ($x = 1$), the Population 2 bacteria at $x = 0.5$ experiencing the highest levels of Population 1 AIP.

3.2 Smaller diffusion, $D = 0.1$

As would be anticipated, if the AIP have smaller diffusion coefficients, a larger value of N is required in each case to ensure Population 2 does not finish up-regulated, see Figure 6, since AIP transport is more limited. For the most part, the bacteria behave in the same way as for when $D = 0.5$, except the transformation from up-regulated to down-regulated is a slightly slower process and inhomogeneities in Population 2 are more evident. The principal difference is that there is now a range of N in which Population 2 can finish partially down-regulated and partially up-regulated, those nearest to the opposition bacteria being the inactive bacteria; in other words, for slow enough diffusion, and depending on the initial conditions and on the value of N, the lack of penetration of signal molecules into Population 2 can leave it in effect split into two subpopulations. In a continuum framework, in between the two subpopulations there must always be a transition layer with intermediate activation levels; the cells in this layer could be viewed as being ready to switch either way with a slight alteration in the conditions of the system.

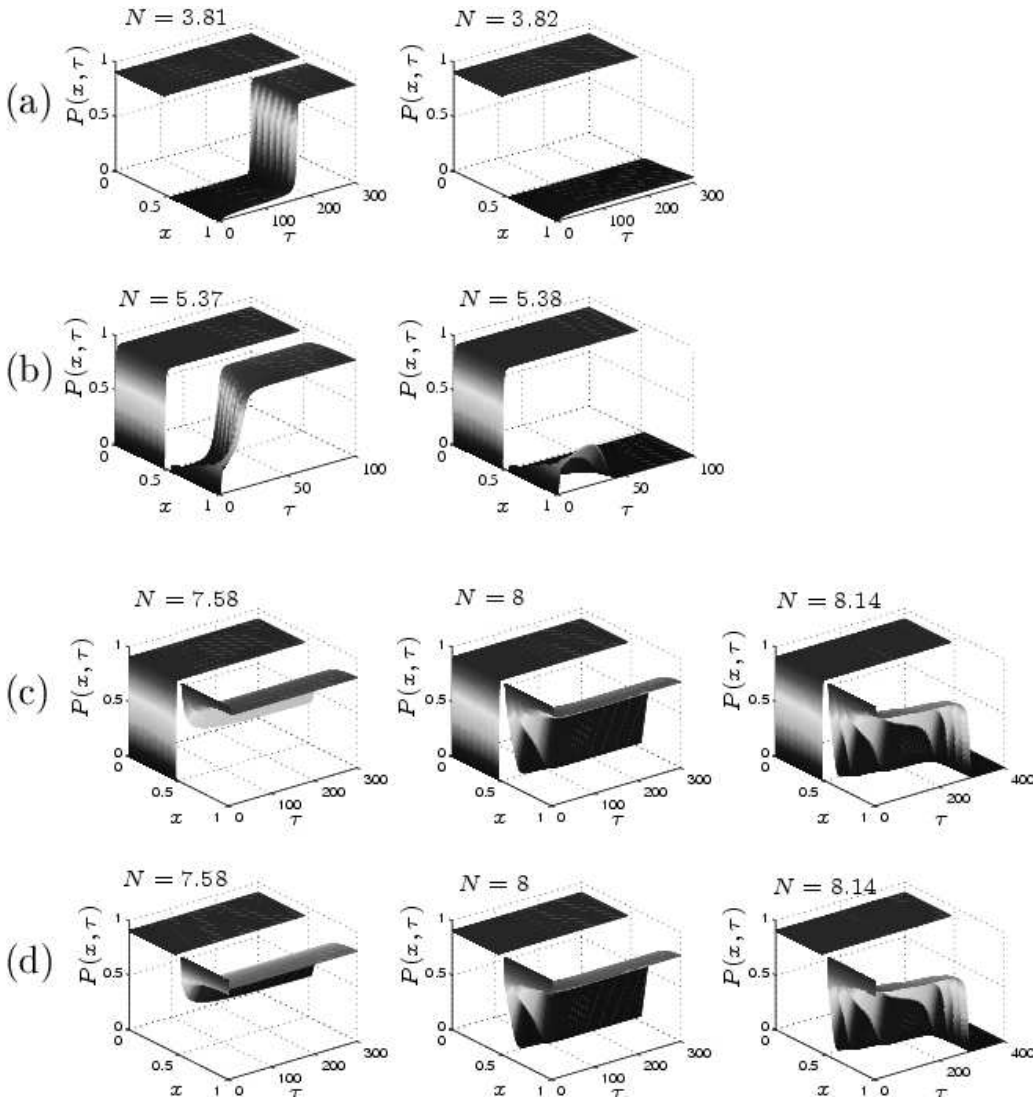

Figure 6: These figures demonstrate, for $D_1 = D_2 = 0.1$, the critical values of N above which, with initial conditions (a) I (b) II (c) III and (d) IV, Population 2 will finish in a down-regulated state. In (a) and (b), as in Figure 5, we infer that Population 1 will gain an advantage by initially already being active. In (c) and (d) we see that taking this smaller diffusion constant results in an extra aspect in the dynamics of the system for initial conditions III and IV: there is now an intermediate range of N in which the Population 2 cells are spatially highly inhomogeneous, with those closest to the opposition cells being forced into a down-regulated state and those furthest away maintaining their active state (in Figure 7 we illustrate this solution for initial condition III with a larger number of grid points in order to demonstrate that this behaviour is not a result of the relatively low number used here).

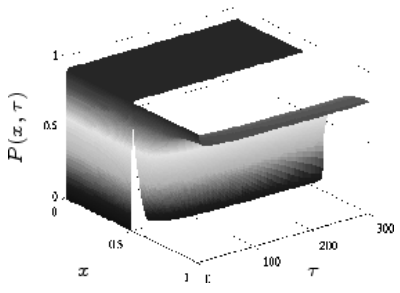

Figure 7: Numerical solution for $P(x,\tau)$ using $D_1 = D_2 = 0.1$, $N = 8$ and initial conditions III (cf. Figure 6(c)), with 801 grid points, i.e. we have divided the populations into many more compartments in order to demonstrate that the ability of the cells to decouple into two subpopulations is not as a result of the relatively low number of compartments used in Figure 6.

4 Steady-state studies

4.1 Preliminaries

The simulations above were performed with a rather crude spatial discretisation, whereby in Figures 5 and 6 we had sixteen compartments or mesh points (this value was chosen to match the number of compartments with the maximum number of equations which can be treated by XPPAUT 5.91 in the subsequent bifurcation analyses). Figure 7 is included to confirm that this relatively low number of spatial compartments does not significantly influence the qualitative properties. Rather than looking at the continuum limit of the discretisation, we now focus explicitly on the compartmentalised version of the model in order to clarify (in the context of this finite-dimensional dynamical system) the bifurcation properties that are implicit in the discussion of §3, i.e. we illustrate various steady state curves at each mesh point (representing a compartment of the population). In all bifurcation diagrams solid lines represent stable steady states and dotted lines unstable ones.

4.2 Larger diffusion, $D = 0.5$

Figure 8 illustrates the solution curves for the equations representing the regulation of Population 2 in each compartment, for varying N, constructed using XPPAUT 5.91. The number of troughs on the unstable curves corresponds to the number of compartments. Due to the limitations of our XPPAUT-based approach, we are

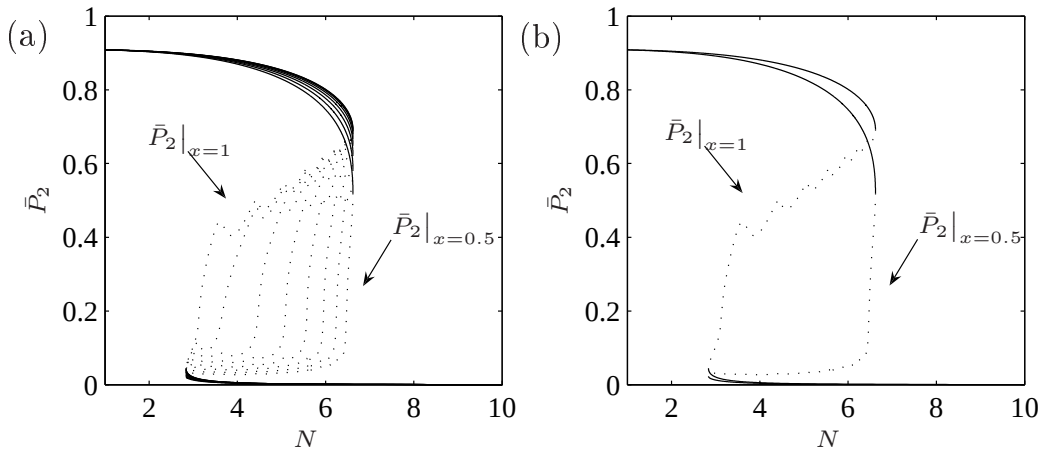

Figure 8: (a) Bifurcation curves for $\bar{P}_2$ with $D_1 = D_2 = 0.5$ for each of the eight compartments in $0.5 \leq x \leq 1$. In (b), for clarity, only the compartments at the extremeties are shown. Each compartment exhibits two fold bifurcations, with the main differences being in where the unstable branch lies: for the compartments close to the opposition cells the unstable branch is much lower than those which are further away in these projections of the bifurcation curve. Solution curves are given only for $N \geq 1$, so that Population 1 is equal or larger in size than Population 2; for $N < 1$ the roles of Populations 1 and 2 are reversed.

unable to investigate what occurs for much larger numbers of compartments and it is therefore unclear whether the troughs are real or an artifact of the low number of mesh points in our discretisation. Given that the troughs affect only the *unstable* steady states, however, they are unlikely to be amenable to useful physical interpretation; though they can be linked to the ability of the population to subdivide for sufficiently small diffusion constants and this will be addressed in §4.3.

Varying N produces a hysteresis similar to that seen in the well-mixed ODE model [18]. A range of N exists in which there are two stable solutions, the 'borderline' between which is given by an unstable one: here the ultimate regulation of Population 2 is dependent upon the initial conditions of the system, confirming what we have seen so far in both the time-dependent solutions in this paper and also in the spatially homogeneous model of Part 1 [18]. Much of what has been discussed for the well-mixed model, therefore, also applies to this spatially structured one. A notable addition, however, is that, while there is only a small difference between the stable solutions of each compartment (those nearest to the Population 1 cells having a slightly lower regulation level than those further away) the unstable curves are significantly different, thus emphasising the importance

of the initial conditions, given the borderline role of the unstable solutions. This remark requires clarification, however, given this spatially structured context, the three solutions cannot be ordered in a simple way within every compartment for every variable: the unstable branch does not always lie between the two stable ones, see Figure 16 in the appendix. Additionally, distances between states in Figure 8 are not necessarily truly reflective of the distances in the full state-space. Nevertheless, the unstable branches do provide a rough guide to the domains of attraction of the system. In order to see this, we begin all variables, except P_2, on the unstable branch, and determine which values of $P_2(x,0)$ will bias the variables towards either the active or inactive state (assuming, for simplicity, that $P_2(x,0)$ is constant over $0.5 \leq x \leq 1$). Since, in the bistable region, the down-regulated stable branch has a smaller area between it and the unstable branch for most compartments, we expect the range of $P_2(x,0)$ which produces the down-regulated state to be smaller than the range which has the opposite effect. Figure 9(a) illustrates a numerical solution to the system when the initial conditions of all the variables (including P_2) are taken from the unstable steady state with $N = 5.00465$ – see Figure 8 (meaning that the initial values of all variables vary across the intervals [0 1/2] and [1/2 1]). We note that the slightly odd choice of N for these simulations stems from the available data generated from our program in XPPAUT 5.91. If these unstable steady states are used, Population 2 is inactivated. Figure 9(b) demonstrates that changing $P_2(x,0)$ to

$$P_2(x,0) = \begin{cases} 0, & 0 \leq x \leq 1/2, \\ 0.302, & 1/2 \leq x \leq 1, \end{cases} \tag{16}$$

results in the suppression of Population 2 into an inactive state. Increasing $P_2(x,0)$, however, to

$$P_2(x,0) = \begin{cases} 0, & 0 \leq x \leq 1/2, \\ 0.303, & 1/2 \leq x \leq 1, \end{cases} \tag{17}$$

(see Figure 9(c)) gives Population 2 enough strength to induce itself into an up-regulated state in spite of the Population 1 AIP. Thus, if all the other variables begin at their unstable steady state, we can assume that for $0 \leq P_2(x,0) \lesssim 0.303$ (for $0.5 \leq x \leq 1$) the population will be drawn towards the down-regulated state, whereas $0.303 \lesssim P_2(x,0) \leq 1$ (again for $0.5 \leq x \leq 1$) will lead to the up-regulated state. For reference, the above simulations for all variables are provided in the appendix.

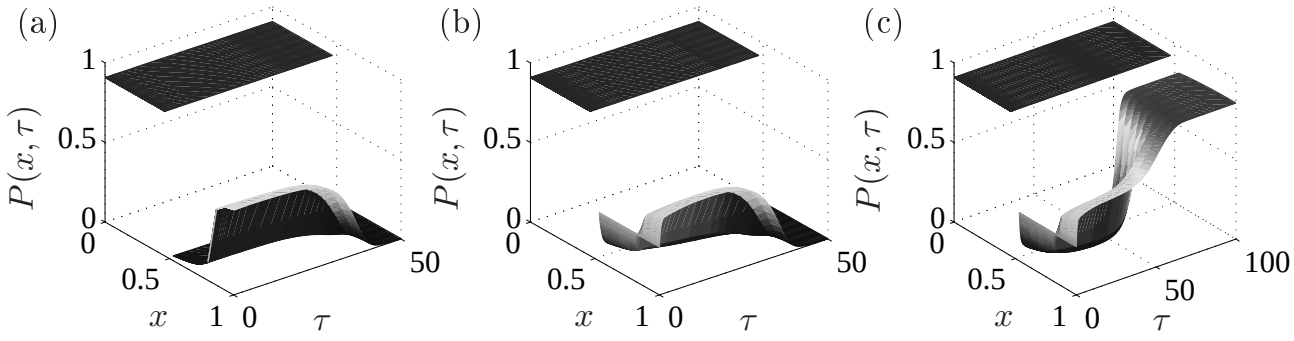

Figure 9: The numerical solution to (2)-(13), using $N = 5.00465$ and taking the initial condition of the system to be the corresponding unstable steady state (a) for all variables, (b) for all the variables except P_2, for which we use (16), (c) for all the variables except P_2, for which we use (17). In (a) the variables remain at the unstable state for a time, before Population 1 (the larger population) is able to push Population 2 into its down-regulated steady state. In (b) the system moves from its unstable steady state to its stable counterpart which has Population 2 down-regulated, while in (c) the initial condition of P_2 is large enough to push its population into an active state alongside Population 1. Comparison between (b) and (c) allows us to infer that any starting value of P_2 less than 0.302 will also result in Population 2 reaching its inactive steady state if all other variables begin at their unstable steady state. The change in Population 1 is not visible on these graphs as the difference between its unstable and stable states is very slight.

4.3 Smaller diffusion, $D = 0.1$

The bifurcation diagram in Figure 10 allows us to see clearly the division into two subpopulations, as introduced in §3.2. Within a specific range of N there are three potential (stable) outcomes: either both populations will finish in an up-regulated state, Population 1 in an up-regulated state and Population 2 down-regulated, or Population 1 in an up-regulated state and Population 2 divided into one active and one inactive subpopulation. Which of these occurs is dependent upon the initial conditions of the system. On the sections of the solution curve which cover the latter steady state, we no longer have the troughs which were discussed in §3.1. Instead these are replaced by two fold (saddle-node) bifurcations. Each of these corresponds to one more compartment of Population 2 having a down-regulated stable steady-state within the subpopulation, so that the troughs are in effect replaced by the cells being able to divide into two subpopulations (possibly explaining why the number of troughs is equal to the number of compartments). On the basis of the numerical results, it seems that there is a limit, however, on the number of compartments that can form the subpopulations. In this example, if an active subpopulation exists, it must consist of a minimum of half of the compartments: a smaller subpopulation will be necessarily down-regulated by the invading AIP (this is another illustration of the natural importance of population size in QS).

We should consider the possible effects of pinning on the solutions of our partial differential equation system. Pinning can occur when the step size used for the spatial discretisation of the system is not sufficiently small, effectively creating additional stable solutions that cannot occur in the continuum limit (for further information about pinning see, for example, [25–29]). Thus, while we have shown in Figure 7 that Population 2 *can* be split into two subpopulations for a much smaller step size than used in Figure 10, it is possible that at steady state, there is in the continuum version of the problem only one possibility for the number of cells in each subpopulation as opposed to the multiple ones illustrated in Figure 10.

As we saw for $D = 0.5$, there is again a wide gap between the unstable branches for each component which again suggests a broader domain of attraction to the up-regulated stable state for Population 2, in the bistable region, than to the down-regulated one.

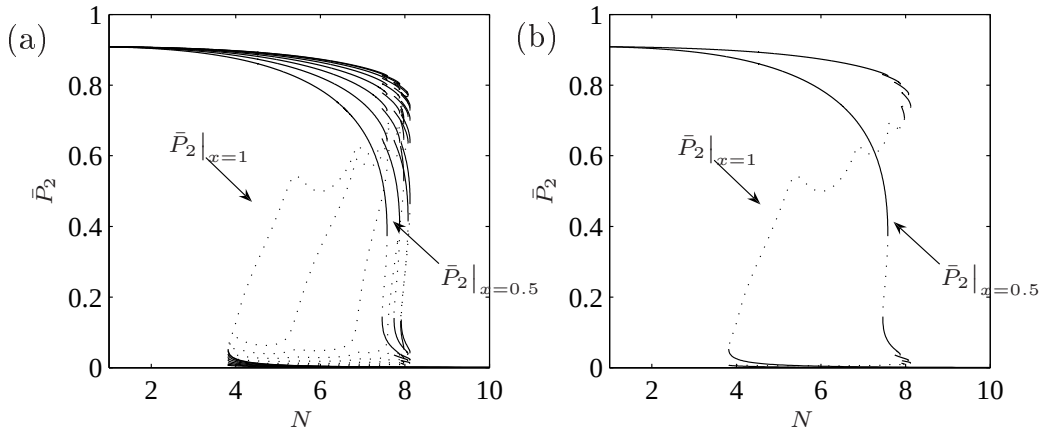

Figure 10: As in Figure 8 we provide the solution curves of $\bar{P}_2$ with varying N for each compartment, now with $D_1 = D_2 = 0.1$. Figure 10(b) shows only the behaviour of $\bar{P}_2$ at the extremities. This smaller diffusion coefficient results in a range of N where the Population 2 cells have an additional aspect to their behaviour, not seen for larger diffusion. They are now capable of essentially being decoupled into two subpopulations. The subpopulation adjacent to the Population 1 cells comes into contact with too much AIP from these opposition cells and not enough from its own cells to become active. At the same time, not enough of the Population 1 AIP is able to reach the subpopulation which is further away (towards $x = 1$) and as such this set of cells is able to use its own AIP to upregulate itself.

5 The significance of the diffusion coefficient

5.1 Preliminaries

Following our investigations in §3 and §4, we see that the diffusion coefficient plays an important role in the dynamics of the system. For the larger coefficient, $D = 0.5$, there are only two real possibilities for the outcome of the Population 2 cells, they will either all be up-regulated or all forced into a down-regulated state by the Population 1 cells. However, for smaller diffusion, $D = 0.1$, the Population 2 cells could be divided into two subpopulations, one being down-regulated and one up-regulated. Our numerical analyses indicate that the influence of the diffusion coefficient varies with N and two different scenarios exist: (i) when the populations are of equal sizes and (ii) when Population 1 is significantly larger than Population 2 (if Population 1 is not significantly larger, the results are the same as for (i)). For the most part, we continue our assumption that the diffusion coefficient is the same for both strains, i.e. $D_1 = D_2 = D$, but in §5.4 the possibility that the two coefficients differ is also explored.

5.2 Equal population sizes

From the results discussed earlier, it would be reasonable to expect that a larger diffusion coefficient would be beneficial to the bacteria. One might anticipate that the ability to spread signal molecules out further (but remaining in the immediate surroundings) would be an advantage. However, it is evident from Figure 11 that this is not always the case (this also allows us to see what happens for values of D larger than 0.5). When the population sizes are equal, increasing the diffusion coefficient ($D_1 = D_2 = D$) actually has a slightly detrimental effect on both populations. This occurs because, if both populations are going to inevitably reach an active state, it is inefficient to lose any AIP to the other strain.

5.3 Population 1 is significantly larger than Population 2

The role of the diffusion constant changes as Population 1 is made to be larger than Population 2, but it must be substantially larger, otherwise the effect of altering D is much the same as when the population sizes are equal. Figure 12 demonstrates the solution curve for each compartment of P_2 as we vary D, for $N = 8$. For sufficiently small D, both strains will be up-regulated. If D is increased slightly, the Population 2 compartments closest to

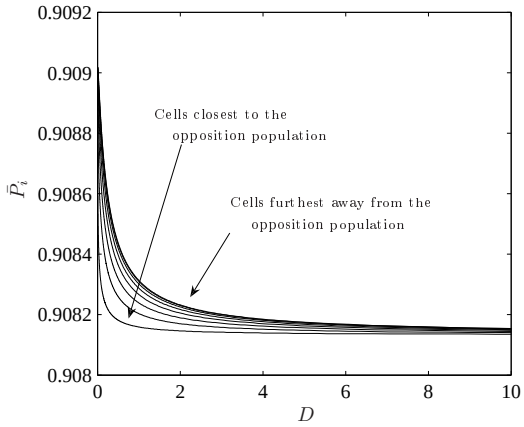

Figure 11: When the population sizes are equal, i.e. $N = 1$, although the difference is not great, it is more efficient for the cells to have AIP molecules which diffuse as little as possible as it is wasteful to lose any when both populations, being equally large, will ultimately upregulate theirselves regardless. Since $N = 1$, the solution curves for both populations are equivalent.

the opposition cells can be downregulated, while those further away can be either active or inactive depending on the initial conditions. As D increases further, more compartments can become inactive, until eventually the only option is that all of Population 2 is forced into a down-regulated state.

The above illustrates that a competing strain may only be able to use a higher diffusion constant in its favour if it is already at an advantage by being the larger population (in which case retaining their own AIP for upregulation is less urgent), assuming that all other factors are equal for the two populations. A smaller diffusion coefficient will be advantageous to the smaller strain as, if sufficiently small, it may enable the bacteria to either gain an active state regardless of its population size, or at least decouple itself so that some of the population can become up-regulated, leaving it in a better position to continue the struggle between the two strains. This is because if the two types of AIP both have a small diffusion constant then Population 2 will not only preserve more of its own AIP for upregulation, but will also come into contact with fewer of the opposition AIP.

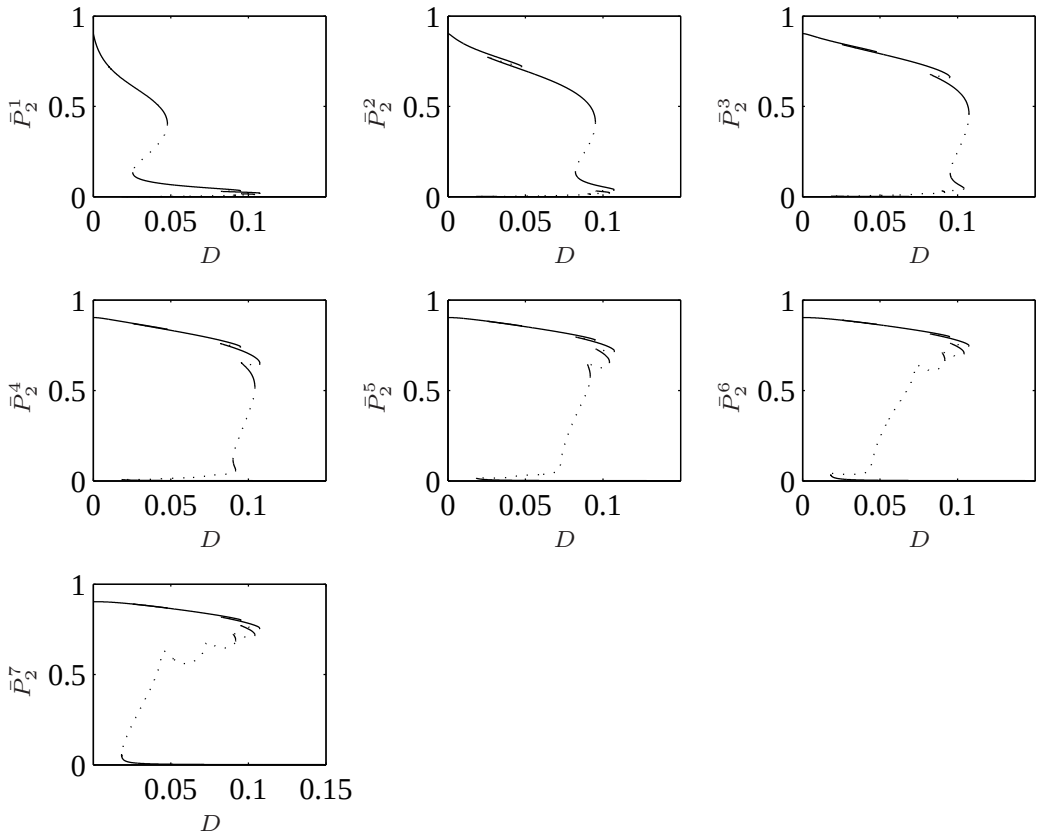

Figure 12: The solution curves for each compartment of P_2 as we vary D, when $N = 8$ and $J = 7$ (notice that we have used fewer compartments in this simulation in order to simplify the numerical calculations). $\bar{P}_2^1$ is the compartment closest to the Population 1 cells, and $\bar{P}_2^7$ is the furthest away. As D increases we see the effect filtering through the population. Initially only the first cells are affected but when D is sufficiently large all the cells are pushed into a down-regulated state.

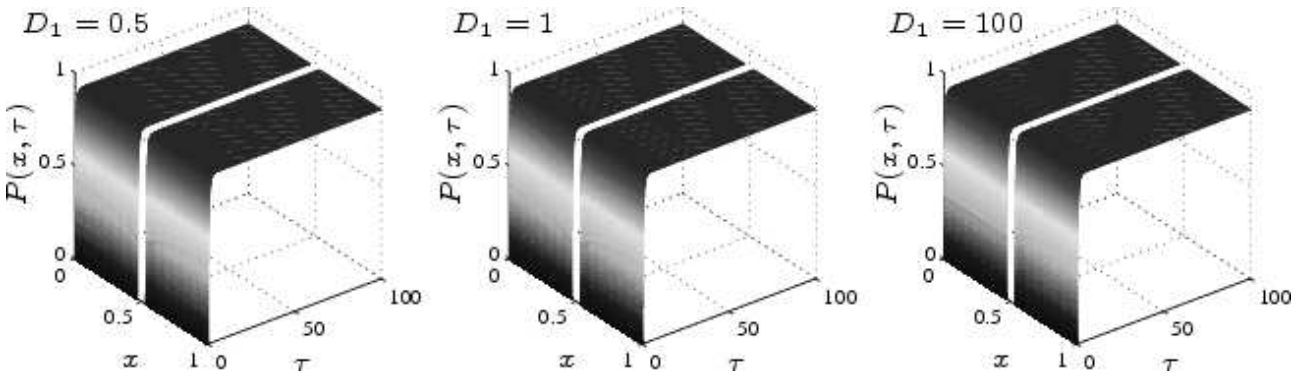

Figure 13: The numerical solution using $N = 1$, $D_2 = 0.5$, various values of D_1 (as stated above each graph) and all the remaining parameters taken from Table 2. When both populations are of equal size they will reach an active state. Hence Population 1 gains no advantage through having a larger AIP diffusion coefficient than Population 2.

5.4 Unequal diffusion coefficients

We have so far only examined the possibility that the two different types of AIP have equal diffusion coefficients. This is a reasonable assumption given their structural similarities. However, we now briefly examine how the cells' behaviour would be affected if the AIPs have different diffusion coefficients, both because evolutionary pressure could drive an alteration in AIP size if this would allow a strain to compete more efficiently with other strains and because it may be possible to specify (at least to an extent) the diffusivity of the AIP of a 'designer' strain.

We begin by examining what happens if the population sizes are equal ($N = 1$) but the Population 1 AIP has a larger diffusion coefficient than the Population 2 AIP, see Figure 13. The results are very similar to those seen in §5.2: both populations ultimately reach an up-regulated state regardless of the value of D_1, and, if anything, it is slightly detrimental for Population 1 to have too large a diffusion coefficient (although this difference is not visible on the graphs) as it is wasteful to lose any AIP to the opposition bacteria.

Secondly, we look at what happens when Population 1 is larger than Population 2 and $D_1 > D_2$. In this case it is beneficial for the Population 1 AIP to have a larger diffusion coefficient, contrast Figure 14 with Figure 5: the critical value of N required for Population 1 to inactivate Population 2 is smaller than that required if $D_1 = D_2$. Thus, if Population 1 already has the advantage through being the larger population then it can use

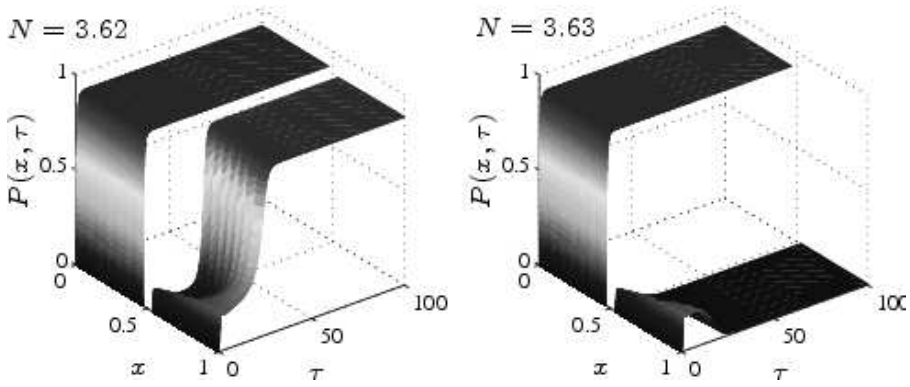

Figure 14: Numerical solutions illustrating the critical value of N required for Population 1 to inactivate Population 2 with $D_1 = 1$, $D_2 = 0.5$, all remaining parameters taken from Table 2 and the initial conditions for the two populations both being the down-regulated state given by (15). If we contrast these results with Figure 5 we see that Population 1 is able to downregulate Population 2 with lower values of N if it has a larger AIP diffusion coefficient than Population 2.

a larger diffusion constant in its favour. Hence, these results for $D_1 \neq D_2$ are analogous to those derived in §5.2 and §5.3, i.e. when $D_1 = D_2 = D$.

Lastly, we examine the situation when Population 1 is larger than Population 2, but has a smaller AIP diffusion coefficient. Comparing Figure 15 with Figures 5 and 14 we see that, with a smaller diffusion coefficient it is harder for the larger population to inhibit the opposition cells because it needs a larger number of cells to produce enough AIP in order for the equivalent amount to be diffused into the opposition territory.

6 Discussion

The diffusion constant plays a crucial role in QS and can be instrumental in establishing the context of the QS. While QS is best understood as a mechanism by which bacteria can sense their population size, it can also be manipulated to recognise their surroundings [4]. The relevance of the diffusion constant (and also the actual size of the bacterial cell) in this context of quorum versus diffusion sensing is discussed by Müller *et al.* [30] in the context of their mathematical model of QS. We recall that the diffusion constant is determined not only by the signal molecule size and structure, but also by the medium in which the bacteria reside, meaning that QS

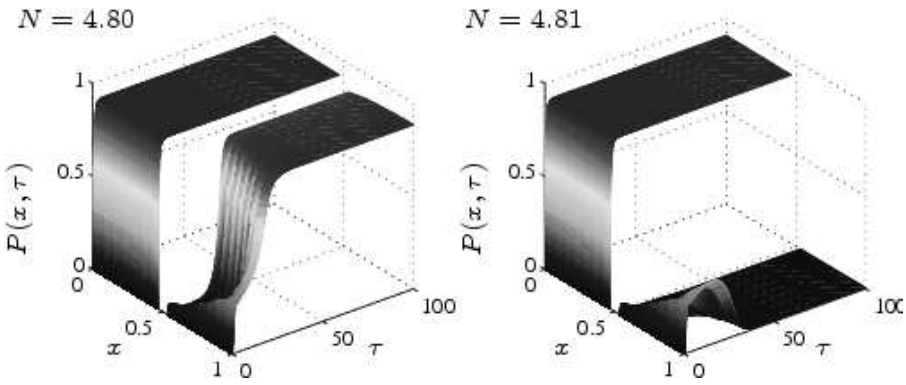

Figure 15: Numerical solutions illustrating the critical value of N required for Population 1 to inactivate Population 2 with $D_1 = 0.1$, $D_2 = 0.5$ and all remaining parameters taken from Table 2. If we contrast these results with Figure 5 we see that higher values of N are required for Population 1 to downregulate Population 2 than when their AIP-diffusion coefficients were equal.

should allow bacteria to sense their environment (for example in endosome escape by *S. aureus*).

In this paper we have illustrated the importance of the diffusion coefficient in terms of the cross-strain QS inhibition in *S. aureus*. From the point of view of the strain present in larger numbers, and thus the dominant strain, it is desirable to be in an environment where the diffusion coefficient is large. From the opposing side, i.e. the strain which is attempting to defend itself from *agr*-suppression, it is preferable for its AIP to have a small diffusion coefficient, hence at least providing the smaller strain with the opportunity to divide into two subpopulations, leaving one inactive and the other active. This is in agreement with the idea that genetic feedback regulation gives a population of cells the ability to behave in a multi-stable fashion [31]: the subpopulation most suited to a particular environmental challenge will survive. The bacteria can afford to lose relatively large amounts of their own AIP to the opposition bacteria (as a result of a large diffusion coefficient) only if they are already the strain more likely to attain *agr* up-regulation, i.e. by being the larger population. In all cases, however (and following results of Part 1 of this study [18]), the most important factor is N, the relative population size. If one population is sufficiently larger than its counterpart, the latter will always be suppressed. This occurs regardless of initial conditions or diffusion constants. In a more general context, both the time-dependent and steady-state investigations shed light upon the variety of spatial patterns which can arise in two competing nonlinear systems of this type.

The mathematical model presented in this study is naturally much more simple than what occurs in reality but it provides an important early step from which to build further analyses of spatially-structured competitive Gram-positive QS systems. The effect of boundary conditions upon the model results is evidently something to be considered in future work. We have assumed that the AIPs are contained within the immediate environment of the bacteria but the results could alter if they were allowed to diffuse away from the bacteria, thus making it harder for a population of bacteria to both upregulate itself and possibly downregulate an opposition population. It is likely that a more pronounced difference in population size would be required in this scenario to guarantee that one population dominates. In addition, more complex spatial configurations should be investigated to better reflect an infection site including inhomogeneous population density distribution (in this situation the diffusion coefficient of the QSSMs may be even more influential).

If a non-pathogenic staphylococcal strain is to be engineered to be used as an anti-staphylococcal therapy, it is important to understand fully the mechanisms by which the bacteria become active in terms of virulence. The results presented in this study shed light upon how the diffusion coefficient of the QSSMs and the relative population size can affect the ability of one population to inactivate the *agr* system of an opposition bacteria. In terms of designing a strain for therapeutic purposes it is important to consider the environment into which this strain is to be administered, the diffusivity of its QSSM (which to a limited extent can be controlled through the strain design) and the maximum possible dosage. Results such as those presented in both parts of this study could provide insight into those choices that would be most likely to ensure that the therapy is successful.

Acknowledgements

SJ gratefully acknowledges support from BBSRC (in the form of a studentship and subsequent funding under the SysMO and SysMO2 initiatives) and from MRC (Biomedical Informatics Fellowship). The remaining authors thank MRC/EPSRC for support. JRK also thanks the Royal Society and Wolfson Foundation for funding.

References

[1] Henke J.M., Bassler B.L. (2004) Bacterial social engagements. *Trends Cell Biol.,* 14, 648–656.

[2] Reading N.C., Sperandio V. (2006) Quorum sensing: the many languages of bacteria. *FEMS Microbiol. Lett.,* 254, 1–11.

[3] Waters C.M., Bassler B.L. (2005) Quorum sensing: cell-to-cell communication in bacteria. *Annu. Rev. Cell. Dev. Biol.,* 21, 319–346.

[4] Redfield R.J. (2002) Is quorum sensing a side effect of diffusion sensing?. *Trends Microbiol.,* 10, 365–370.

[5] Hense B.A., Kuttler C., Müller J., Rothballer M., Hartmann A., Kreft J. (2007) Does efficiency sensing unify diffusion and quorum sensing?. *Nature Rev. Mirobiol.,* 5, 230–239.

[6] Alberghini S., Polone E., Corich V., Carlot M., Seno F., Trovato A., Squartini A. (2009) Consequences of relative cellular positioning on quorum sensing and bacterial cell-to-cell communication. *FEMS Microbiol. Lett.,* 292, 149–161.

[7] Novick R.P. (2003) Autoinduction and signal transduction in the regulation of staphylococcal virulence. *Mol. Microbiol.,* 48, 1429–1449.

[8] Salmond G.P.C., Bycroft B.W., Stewart G.S.A.B., Williams P. (1995) The bacterial 'enigma': cracking the code of cell-cell communication. *Mol. Microbiol.,* 16, 615–624.

[9] Koerber A.J., King J.R., Williams P. (2005) Deterministic and stochastic modelling of endosome escape by *Staphylococcus aureus*: 'quorum' sensing by a single bacterium. *J. Math. Biol.,* 50, 440–488.

[10] Qazi S., Middleton B., Muharram S.H., Cockayne A., Hill P., O'Shea P., Chhabra S.R., Cámara M., Williams P. (2006) N-Acylhomoserine lactones antagonize virulence gene expression and quorum sensing in *Staphylococcus aureus*. *Infect. Immun.,* 74, 910–919.

[11] Ji G., Beavis R., Novick R.P. (1997) Bacterial interference caused by autoinducing peptide variants. *Science,* 276, 2027–2030.

[12] Sebaihia M., Peck M.W., Minton N.P. *et al.* (2007) Genome sequence of a proteolytic (Group I) *Clostridium botulinum* strain Hall A and comparative analysis of the clostridial genomes. *Genome Res.,* 17, 1082–1092.

[13] Ohtani K., Yuan Y., Hassan S., Wang R., Wang Y., Shimizu T. (2009) Virulence gene regulation by the *agr* system in *Clostridium perfringens*. *J. Bacteriol.,* 191, 3919–3927.

[14] Podbielski A., Kreikemeyer B. (2004) Cell density-dependent regulation: basic principles and effects on the virulence of Gram-positive cocci. *Int. J. Infect. Dis.,* 8, 81–95.

[15] Riedel C.U., Monk I.R., Casey P.G., Waidmann M.S., Gahan C.G.M., Hill C. (2009) AgrD-dependent quorum sensing affects biofilm formation, invasion, virulence and global gene expression profiles in *Listeria monocytogenes*. *Mol. Microbiol.,* 71, 1177–1189.

[16] Mayville P., Ji G., Beavis R., Yang H., Goger M., Novick R.P., Muir T.W. (1999) Structure-activity analysis of synthetic autoinducing thiolactone peptides from *Staphylococcus aureus* responsible for virulence. *Proc. Natl. Acad. Sci. USA,* 96, 1218–1223.

[17] Alekshun M.N., Levy S.B. (2004) Targeting virulence to prevent infetion: to kill or not to kill. *Drug Discov. Today,* 1, 483–489.

[18] Jabbari S., King J.R., Williams P. Cross-strain quorum sensing inhibition by *Staphylococcus aureus*. Part 1: a spatially homogeneous model. *Submitted to Bull. Math. Biol. 2011,*.

[19] Anguige K., King J.R., Ward J.P. (2005) Modelling antibiotic- and anti-quorum sensing treatment of a spatially-structured *Pseudomonas aeruginosa* population. *J. Math. Biol.,* 51, 557–594.

[20] Jabbari S., King J.R., Williams P. (2010) A mathematical investigation of the effects of inhibitor therapy on three putative phosphorylation cascades governing the two-component system of the *agr* operon. *Math. Biosci.,* 225, 115–131.

[21] Jabbari S. Mathematical modelling of quorum sensing and its inhibition in *Staphylococcus aureus* PhD thesis University of Nottingham, UK (2007).

[22] Jabbari S., King J.R., Koerber A.J., Williams P. (2010) Mathematical modelling of the *agr* operon in *Staphylococcus aureus*. *J. Math. Biol.,* 61, 17–54.

[23] Gustafsson E., Nilsson P., Karlsson S., Arvidson S. (2004) Characterizing the dynamics of the quorum-sensing system in *Staphylococcus aureus*. *J. Mol. Microbiol. Biotechnol.,* 8, 232–242.

[24] Lyon G.J., Wright J.S., Muir T.W., Novick R.P. (2002) Key determinants of receptor activation in the *agr* autoinducing peptides of *Staphylococcus aureus*. *Biochemistry-US,* 41, 10095–10104.

[25] Carpio A., Bonilla L.L. (2001) Wave front depinning transition in discrete one-dimensional reaction-diffusion systems. *Phys. Rev. Lett,,* 86, 6034–6037.

[26] Elmer C.E., Van Vleck E.S. (1999) Analysis and computation of travelling wave solutions of bistable differential-difference equations. *Nonlinearity,* 12, 771–798.

[27] Keener J.P. (1987) Propagation and its failure in coupled systems of discrete excitable cells. *SIAM J. Appl. Math.,* 47, 556–572.

[28] King J.R., Chapman S.J. (2001) Asymptotics beyond all orders and Stokes lines in nonlinear differential-difference equations. *Eur. J. Appl. Math.,* 12, 433–463.

[29] Kladko K., Mitkov I., Bishop A.R. (2000) Universal scaling of wave propagation failure in arrays of coupled nonlinear cells. *Phys. Rev. Lett.,* 84, 4505–4508.

[30] Müller J., Kuttler C., Hense B.A., Rothballer M., Hartmann A. (2006) Cell-cell communication by quorum sensing and dimension-reduction. *J. Math. Biol.,* 53, 672–702.

[31] Smits W.K., Kuipers O.P., Veening J.W. (2006) Phenotypic variation in bacteria: the role of feedback regulation. *Nature Reviews Microbiol.,* 4, 259–271.

A Simplifying the spatially homogeneous model of [18]

With a view to simplifying our cross-inhibition model, we extend the asymptotic approximations derived in [20] to cover this two-population model. Certain variables are not defined in the main text as they are either eliminated from or taken to be at quasi-steady state in the simplified model. For Population $j = 1, 2$ (with $l = 3-j$), these are B_j (cytoplasmic AgrB), C_j (cytoplasmic AgrC), D_j (cytoplasmic AgrD), T_j (transmembrane AgrB), $R_{P_j}^{a_j}$ (transmembrane AgrC bound to cognate AIP), $R_j^{a_l}$ (transmembrane AgrC bound to opposition AIP) and A_{Pj} (phosphorylated AgrA). Firstly, we note that in the steady state $M_j \equiv B_j \equiv C_j \equiv D_j \equiv T_j$ $(j = 1, 2)$, so that we can immediately eliminate B_j, C_j, D_j and T_j in favour of M_j. We have three principal steady-state situations which we wish to examine.

S.S. I Both populations are up-regulated.

S.S. II Population 1 is up-regulated and Population 2 down-regulated.

S.S. III Population 1 is down-regulated and Population 2 up-regulated.

Assuming that both populations are sufficiently large, we do not consider the possibility that neither population becomes up-regulated. As the latter two are effectively mirror images of each other we only need to look at one of these two to see which terms are required in such a scenario. We therefore only provide the asymptotic approximations to the steady states of the first two cases. We retain the parameter scalings given in [18, 20].

A.1 Steady State I: Both populations are up-regulated

The corresponding variables from each population are scaled in the same manner. Thus, for $j = 1, 2$ and $l = 3 - j$ respectively,

$$R_j = \epsilon^2 {R_j}', \qquad A_j = \epsilon {A_j}', \qquad M_j = \frac{1}{\epsilon} {M_j}', \qquad S_j = \frac{1}{\epsilon} {S_j}',$$
$$A_{Pj} = \frac{1}{\epsilon} {A_{Pj}}', \qquad {R_P}_j^{a_j} = \frac{1}{\epsilon^2} {R_P}_j^{a_j\prime}, \qquad R_j^{a_l} = \frac{1}{\epsilon^2} R_j^{a_l\prime}, \qquad a_j = \frac{1}{\epsilon^4} {a_j}',$$

the steady-state equations (dropping any $'$'s) follow:

$$0 = \hat{\upsilon} P_j - M_j + \epsilon, \tag{18}$$

$$0 = \lambda M_j - \epsilon^2 \lambda A_j - \phi A_j {R_P}_j^{a_j} + \epsilon \hat{\mu} \phi A_{Pj}, \tag{19}$$

$$0 = \lambda (B_1 - S_1) - \hat{k}_S B_1 S_1, \tag{20}$$

$$0 = \lambda (B_2 - S_2) - \frac{\hat{k}_S}{N} B_2 S_2, \tag{21}$$

$$0 = \hat{k}_a B_1 S_1 - \epsilon \hat{\beta}_{11} R_1 a_1 + \epsilon \hat{\beta}_{11} \gamma_{11} {R_P}_1^{a_1} - \epsilon \frac{\hat{\beta}_I \hat{\beta}_{21}}{N} R_2 a_1 + \epsilon \frac{\hat{\beta}_I \hat{\beta}_{21} \gamma_{12}}{N} R_2^{a_1} - \lambda_a a_1, \tag{22}$$

$$0 = \frac{\hat{k}_a \hat{\beta}_A}{N^3} B_2 S_2 - \epsilon \frac{\hat{\beta}_{11} \hat{\beta}_A}{N} R_2 a_2 + \epsilon \frac{\hat{\beta}_{11} \hat{\beta}_A \gamma_{22}}{N} {R_P}_2^{a_2} - \epsilon \hat{\beta}_{21} R_1 a_2 + \epsilon \hat{\beta}_{21} \gamma_{21} R_1^{a_2} - \lambda_a a_2, \tag{23}$$

$$0 = \lambda B_1 - \epsilon^3 \lambda R_1 - \hat{\eta} R_1 a_1 + \hat{\eta} \gamma_1 {R_P}_1^{a_1} - \frac{N \hat{\beta}_{21} \hat{\eta}}{\hat{\beta}_{11} \hat{\beta}_A} R_1 a_2 + \frac{N \hat{\beta}_{21} \hat{\eta} \gamma_{21}}{\hat{\beta}_{11} \hat{\beta}_A} R_1^{a_2}, \tag{24}$$

$$0 = \lambda B_2 - \epsilon \lambda R_2 - N \hat{\eta} R_2 a_2 + N \hat{\eta} \gamma_{22} {R_P}_2^{a_2} - \frac{\beta_I \hat{\beta}_{21} \hat{\eta}}{\hat{\beta}_{11}} R_2 a_1 + \frac{\beta_I \hat{\beta}_{21} \hat{\eta} \gamma_{12}}{\hat{\beta}_{11}} R_2^{a_1}, \tag{25}$$

$$0 = R_j a_j - (\lambda + \gamma_{jj}) {R_P}_j^{a_j}, \tag{26}$$

$$0 = R_j a_l - (\lambda + \gamma_{lj}) R_j^{a_l}, \tag{27}$$

$$0 = A_j {R_P}_j^{a_j} - (\lambda + \epsilon \hat{\mu}) A_{Pj}, \tag{28}$$

$$0 = A_{Pj}(1 - P_j) - \epsilon u P_j. \tag{29}$$

A.2 Steady State II: Population 1 is up-regulated and Population 2 is down-regulated

We now manipulate the up-regulated scalings for Population 1 and the down-regulated ones for Population 2 from [20].

$$R_1 = \epsilon^2 {R_1}', \qquad A_1 = \epsilon {A_1}', \qquad M_1 = \frac{1}{\epsilon} {M_1}', \qquad S_1 = \frac{1}{\epsilon} {S_1}',$$
$$A_{P1} = \frac{1}{\epsilon} {A_{P1}}', \qquad R_{P_1}^{a_1} = \frac{1}{\epsilon^2} {R_{P_1}^{a_1}}', \qquad a_1 = \frac{1}{\epsilon^4} {a_1}',$$

$$R_2 = \epsilon^3 {R_2}', \qquad P_2 = \epsilon {P_2}', \qquad A_{P2} = \epsilon {A_{P2}}', \qquad R_{P_2}^{a_2} = \epsilon {R_{P_2}^{a_2}}', \qquad R_2^{a_1} = \frac{1}{\epsilon} {R_2^{a_1}}', \qquad a_2 = \frac{1}{\epsilon^2} {a_2}'.$$

For the first population, (18)-(20) and (26)-(29) hold ($j = 1, l = 2$), with the only equations which change in this situation being,

$$0 = \hat{k}_a B_1 S_1 - \epsilon \hat{\beta}_{11} R_1 a_1 + \epsilon \hat{\beta}_{11} \gamma_{11} R_{P_1}^{a_1} - \epsilon^2 \frac{\hat{\beta}_I \hat{\beta}_{21}}{N} R_2 a_1 + \epsilon^2 \frac{\beta_I \hat{\beta}_{21} \gamma_{12}}{N} R_2^{a_1} - \lambda_a a_1, \tag{30}$$
$$0 = \lambda B_1 - \epsilon^3 \lambda R_1 - \hat{\eta} R_1 a_1 + \hat{\eta} \gamma_{11} R_{P_1}^{a_1} - \epsilon^2 \frac{N \hat{\beta}_{21} \hat{\eta}}{\hat{\beta}_{11} \hat{\beta}_A} R_1 a_2 + \epsilon^2 \frac{N \hat{\beta}_{21} \hat{\eta} \gamma_{21}}{\hat{\beta}_{11} \hat{\beta}_A} R_1^{a_2}. \tag{31}$$

On the other hand, all but five equations change for Population 2, so that we have (26)-(29) ($j = 2, l = 1$) and,

$$0 = \hat{v} P_2 - M_2 + 1, \tag{32}$$
$$0 = \lambda(M_2 - A_2) - \epsilon \phi A_2 R_{P_2}^{a_2} + \epsilon^2 \hat{\mu} \phi A_{P2}, \tag{33}$$
$$0 = \lambda(B_2 - S_2) - \epsilon \frac{\hat{k}_S}{N} B_2 S_2, \tag{34}$$
$$0 = \frac{\hat{k}_a \hat{\beta}_A}{N^3} B_2 S_2 - \epsilon^2 \frac{\hat{\beta}_{11} \hat{\beta}_A}{N} R_2 a_2 + \epsilon^2 \frac{\hat{\beta}_{11} \hat{\beta}_A \gamma_{22}}{N} R_{P_2}^{a_2} - \epsilon \hat{\beta}_{21} R_1 a_2 + \epsilon \hat{\beta}_{21} \gamma_{21} R_1^{a_2} - \lambda_a a_2, \tag{35}$$
$$0 = \lambda B_2 - \epsilon^3 \lambda R_2 - \epsilon^2 N \hat{\eta} R_2 a_2 + \epsilon^2 N \hat{\eta} \gamma_{22} R_{P_2}^{a_2} - \frac{\hat{\beta}_I \hat{\beta}_{21} \hat{\eta}}{\hat{\beta}_{11}} R_2 a_1 + \frac{\beta_I \hat{\beta}_{21} \hat{\eta} \gamma_{12}}{\hat{\beta}_{11}} R_2^{a_1}, \tag{36}$$
$$0 = A_{P2}(1 - \epsilon P_2) - u P_2. \tag{37}$$

A.3 Resulting simplifications

The equations representing ${R_P}_j^{a_j}$, $R_j^{a_l}$ and A_{Pj} are the same regardless of the regulation level. We thus manipulate equations (26)-(28) to eliminate these variables, i.e. we keep them in quasi-steady state and have

$$ {R_P}_j^{a_j} = \frac{R_j a_j}{(\lambda + \gamma_{jj})}, \qquad R_j^{a_l} = \frac{R_j a_l}{(\lambda + \gamma_{lj})}, \qquad A_{Pj} = \frac{A_j {R_P}_j^{a_j}}{(\lambda + \epsilon\hat{\mu})}. \tag{38} $$

This is equivalent to the assumption that binding and activating reactions are relatively fast. We neglect the housekeeping terms in (19), (28), (33) and (38) (those represented by μ) because this reaction is negligible in relation to either natural depletion or activation of AgrA (which of these latter two reactions dominates is dependent upon the state of the cell). Additionally we neglect the binding and separation reactions in (22), (23), (30) and (35) because production and degradation of AIP dominates, and finally also the degradation terms ($-\lambda R$) in (24), (25), (31) and (36). This last simplification corresponds to the assumption that the sink term controlling receptor levels is given by binding reactions as opposed to degradation. The resulting simplified model is described in the main text.

B Additional numerical solutions

B.1 Steady-state studies

B.1.1 Larger diffusion, $D = 0.5$

We here provide some additional numerical simulations to complement those of §4.2. In Figure 16, we illustrate the complexity of the bifurcation diagrams in multi-variable state space through the projections of these curves for $D = 0.5$ and varying N for A_2. The unstable steady states and lower stable branches are qualitatively very similar to those of P_2 (see Figure 8). The steady states of A corresponding to the inactive stable branch are given by $\bar{A} \sim \hat{v}\bar{P} + 1$ in the asymptotic limit $\epsilon \to 0$ (see Appendix A for all the asymptotic approximations discussed here), so it is clear that the inactive branches of $\bar{A}$ and $\bar{P}$ should be qualitatively equivalent; the fact that the unstable branches also are suggests that the above approximation applies here as well. On the active stable branch, however, AgrA levels, in the limit $\epsilon \to 0$, are determined by a balance between mRNA and AIP-bound receptor concentrations, so that these branches follow a trend quite different to those we have

previously depicted.

B.1.2 Smaller diffusion, $D = 0.1$

The full numerical solutions relating to Figure 9 are depicted in Figures 17-19.

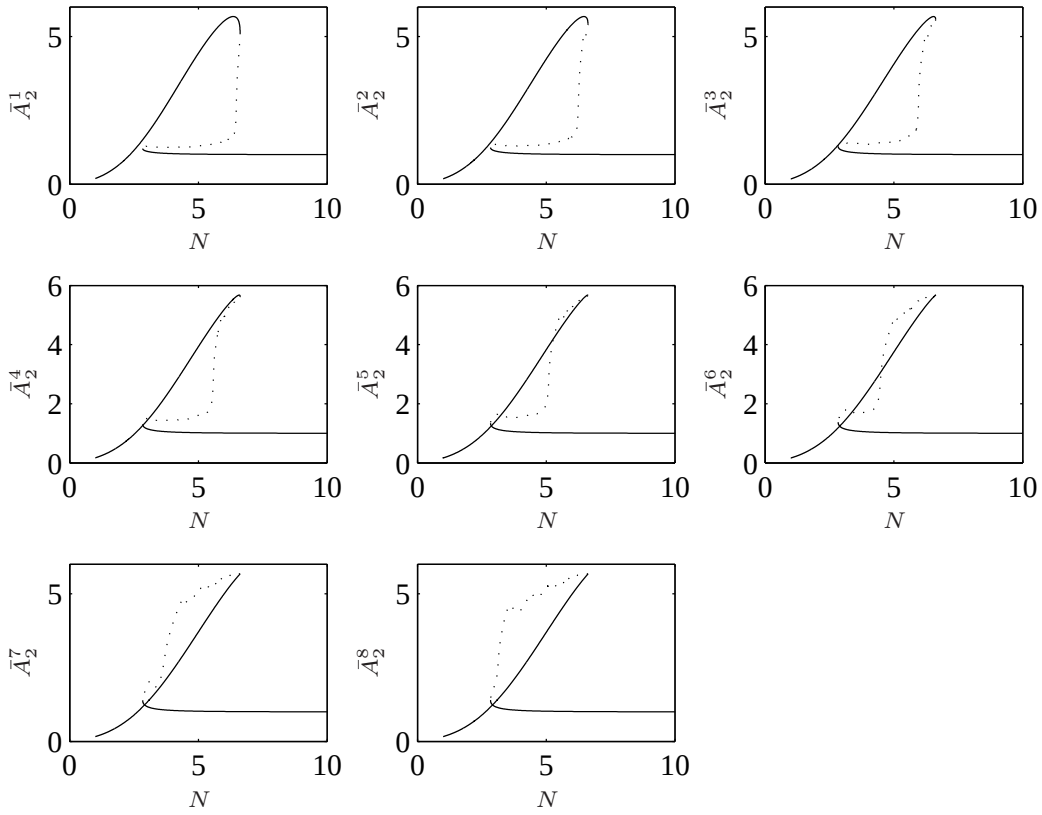

Figure 16: Steady-state solution curves for A_2 (AgrA levels of Population 2), $\bar{A}_2$, for each compartment with varying N, demonstrating the complexity of the nonlinear behaviour. The curve-shape alters part way through the interval when the unstable branch flips over from between the two stable branches (where, remembering previous solution curves, we would probably expect it to lie) to above both branches (the point at which the branches cross in this projection of the A_2 component of the steady state does not correspond to a bifurcation). This behaviour illustrates how complicated the domains of attraction in such a system are likely to be.

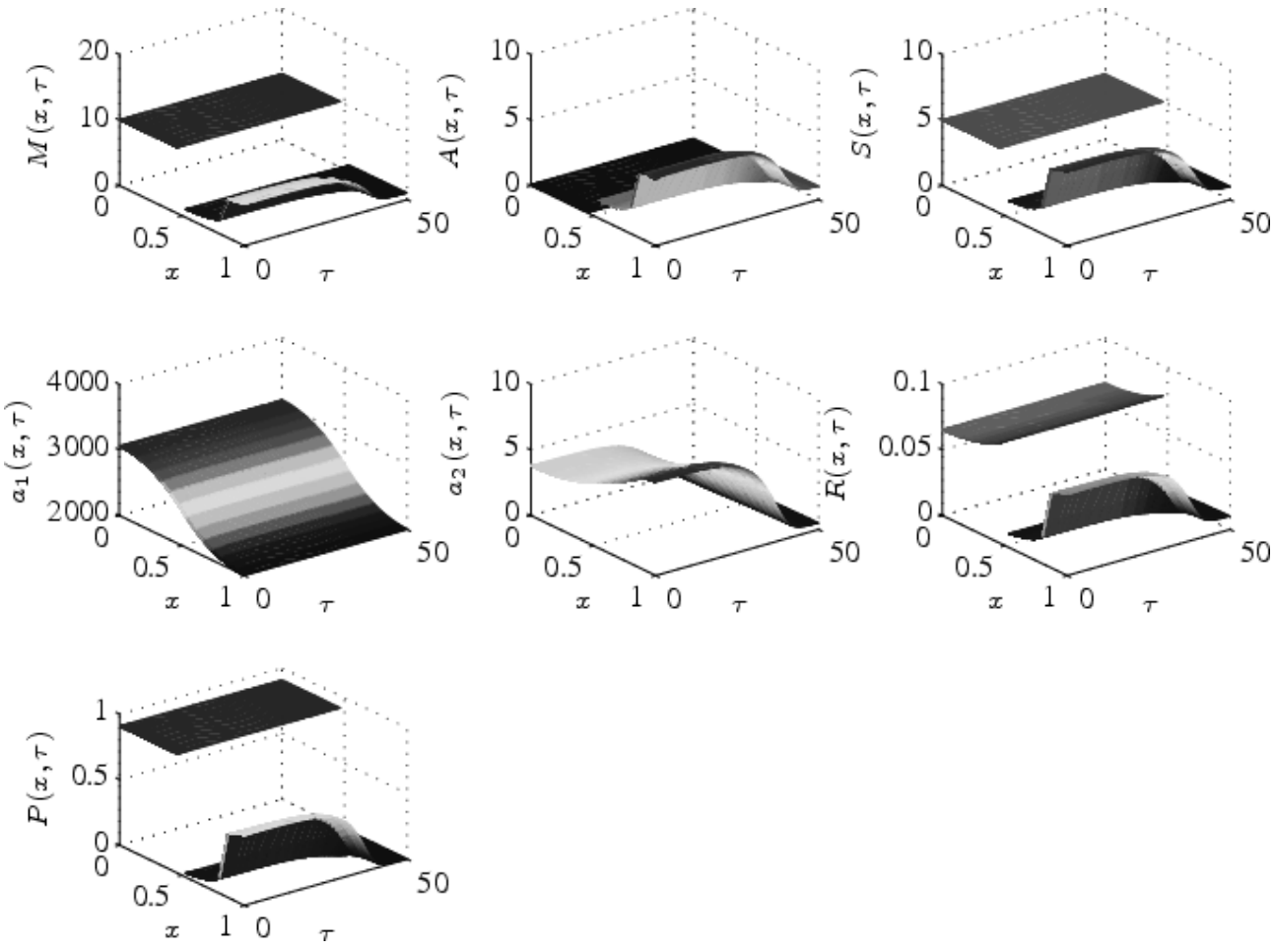

Figure 17: The numerical solution to (2)-(13), using $N = 5.00465$ and the corresponding unstable steady state as the initial condition of the system. The variables remain in this state for a time, before Population 1 (the larger population) is able to push Population 2 into its down-regulated steady state. We note that $A_1(x,t)$ is close to, but not equal to, zero (the same applies to Figures 18 and 19).

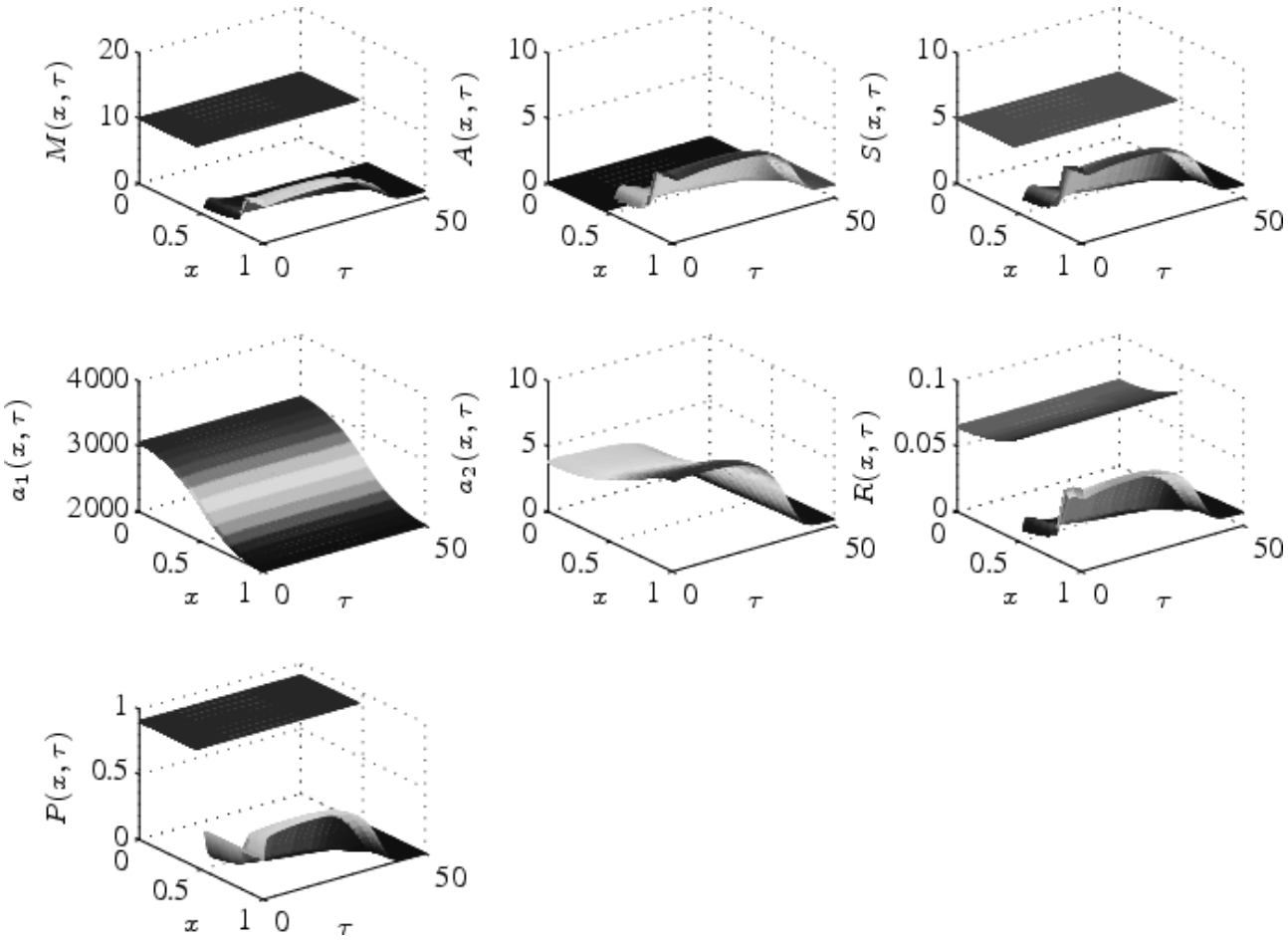

Figure 18: The numerical solution to (2)-(13), using $N = 5.00465$ and the corresponding unstable steady states as the initial conditions for all the variables except P_2, for which we use (16). We see the system moving from the unstable steady state to its down-regulated stable counterpart. Comparison between this solution and that of Figure 19 allows us to infer that any starting value of P_2 less than 0.302 will also result in Population 2 reaching its inactive steady state if all other variables begin at their unstable steady state.

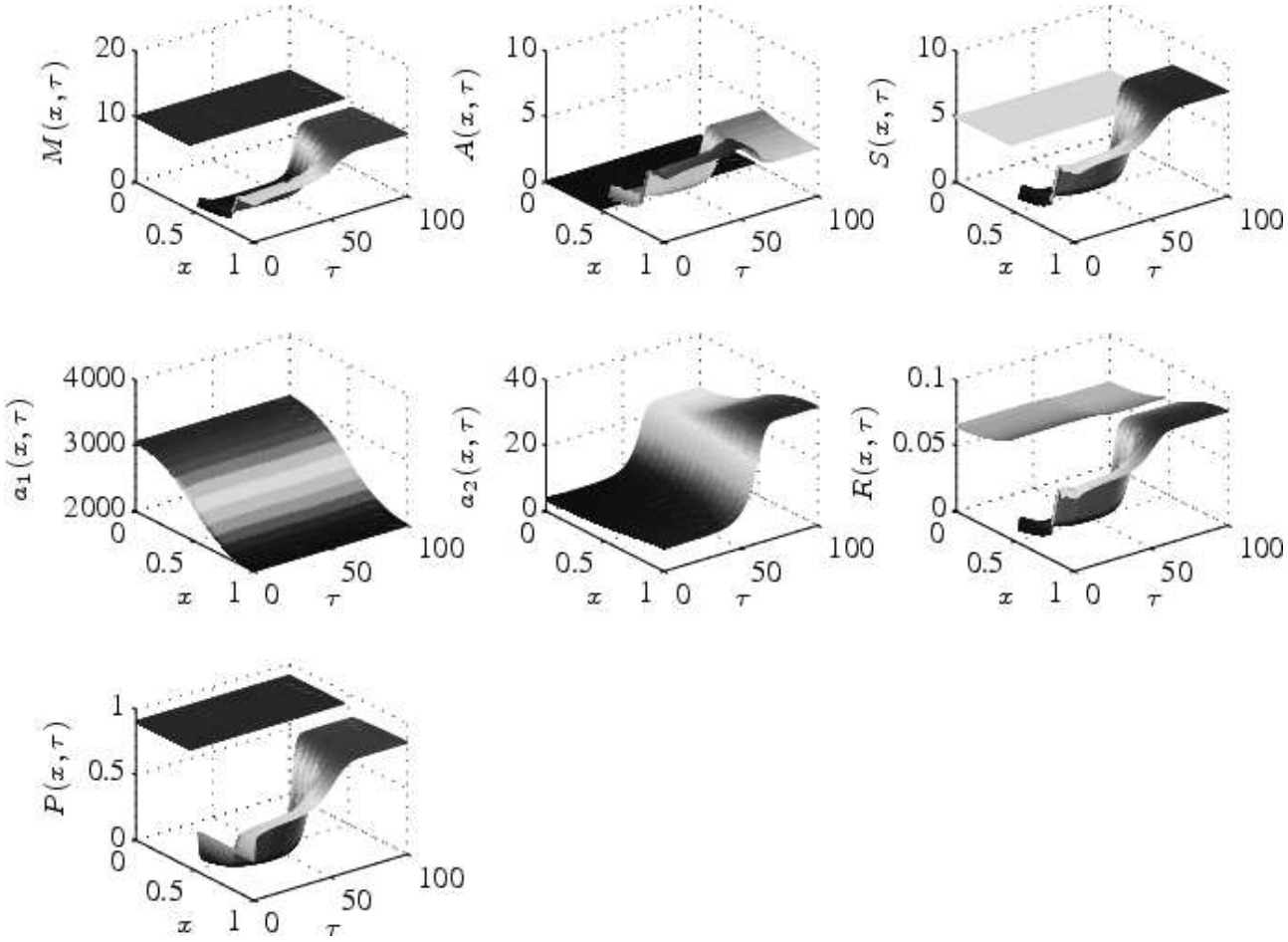

Figure 19: The numerical solution to (2)-(13), using $N = 5.00465$ and the corresponding unstable steady states as the initial conditions for all the variables except P_2, for which we use (17). This extra advantage that Population 2 has from its initial conditions in relation to its cells in Figure 18 allows Population 2 to upregulate itself, and gain an equivalent position to its opponent. The interval of $P_2(x, 0)$ which will therefore allow Population 2 to activate itself is greater than the interval which will cause its cells to be down-regulated (when all other variables begin at their unstable steady state).